

Monitoring of Rain Water Storage in Forests With Satellite Radar

Joost J. M. de Jong, *Student Member, IEEE*, Wim Klaassen, and Pieter J. C. Kuiper

Abstract—The sensitivity of radar backscatter to the amount of intercepted rain in temperate deciduous forests is analyzed to determine the feasibility of retrieval of this parameter from satellite radar data. A backscatter model is validated with X-band radar measurements of a single tree exposed to rain. A good agreement between simulation and measurements is observed and this demonstrates the ability of radar to measure the amount of intercepted rain. The backscatter model is next applied to simulate different satellite radar configurations. To account for forest variability, the backscatter difference between a wet and dry forest canopy is calculated for four deciduous tree species, above a wet and a dry soil. On average, the simulated backscatter of a wet forest canopy is 1 dB higher than the backscatter of a dry forest canopy at co-polarized L-band and 2 dB at co-polarized C and X-band. The simulated sensitivity is in agreement with observations. It is argued that current satellites can retrieve the amount of intercepted rain at best with a reliability of 50%, due to the variability in soil moisture, species composition and system noise. We expect that the reliability will improve with the launch of the next generation radar satellites. The results of this analysis may also be used to assess the influence of rain, fog or dew upon other radar applications for temperate deciduous forests.

Index Terms—Dew, fog, forest, interception, radar, rain.

I. INTRODUCTION

SINCE the launch of the ERS-1 in 1991, imaging satellite radars continuously monitor forests. Examples of products generated from radar images are maps of forest biomass, forest type, tree moisture content, and even soil moisture content and flooding under forest canopies [1]–[4]. Radar images acquired during or just after rain are unsuitable for most applications, because radar backscatter of a forest changes by wetting [5]–[11]. This sensitivity of backscatter to forest wetness may result in a new application of radar images: retrieval of the amount of intercepted rain in the canopies of forests.

A dense forest canopy intercepts most raindrops at the beginning of rainfall. This water is retained as small droplets or as a thin waterfilm upon the surface of leaves and branches [12]. A canopy can retain up to a certain amount of water, the maximum storage capacity. After a rainstorm, stored water quickly evaporates, mostly within hours. A forest canopy is therefore a temporal water reservoir at the surface-atmosphere boundary.

Manuscript received January 19, 2001; revised October 16, 2001. This work was supported in part by the Space Research Organization Netherlands, Grant EO-021.

J. de Jong and P. Kuiper are with the Plant Physiology, Department of Biology, University of Groningen, Haren, The Netherlands (e-mail: j.j.m.de.jong@biol.rug.nl).

W. Klaassen is with the Marine Biology, Department of Biology, University of Groningen, Haren, The Netherlands.

Publisher Item Identifier S 0196-2892(02)01885-5.

This reservoir can also be filled by interception of cloudwater or dew. Both precipitation and maximum storage capacity are distributed spatially heterogeneous. The dynamic and spatially heterogeneous behavior results in large uncertainties in the quantification of rainfall interception [13]–[15]. It was, for example, demonstrated that the modeled Amazon basin surface-climatology would change from a run-off dominated to an evaporation dominated regime by ignoring spatial heterogeneity of rainfall. Other theoretical studies have shown that the interception loss of precipitation calculated with spatially averaged parameters deviates a factor three to four with the interception loss calculated with detailed models accounting for heterogeneity [16], [17]. An adequate representation of the hydrological balance at the land surface is one of the main uncertainties in global climate simulations [18]. A snapshot of the spatial distribution of rainwater storage could provide data to determine spatially averaged interception, which in turn can be used to tune large-scale climatological, meteorological and hydrological models.

Whether the amount of rainwater storage can be measured by radar, depends upon the sensitivity of radar backscatter to storage. Scarce reports give insight into the backscatter processes when a forest becomes wet. Shortly after rain, the backscatter of a mixed forest increased with 0 dB at P-band (0.44 GHz), with 1–2 dB at L-band (1.25 GHz) and with 2–3 dB at C-band (5.26 GHz), for all polarization directions [7], demonstrating that the radar sensitivity to storage of rainwater depends upon the radar frequency. Forest type also influences the backscatter change after rain. The rain induced C-band backscatter increase of nearby deciduous and coniferous stands was 2 dB and 1 dB in Alaska [9] and 1.5 dB and 0.9 dB in France [10], respectively. For the same amount of rainwater storage in the canopy, model simulations resulted in a stronger backscatter increase for deciduous forest than for coniferous forest [11]. Therefore, the stronger backscatter increase of wet deciduous stands was probably caused by the difference in forest structure. The maximum sensitivity of radar backscatter to storage and how this depends on the radar properties and forest structure, remains uncertain due to the limited number of reported observations.

The objective of this study is to determine the potential of present and future imaging satellite radars for storage retrieval, or in other words: is the maximum radar sensitivity to storage large enough to enable storage retrieval from radar data? To answer this question, the relation between radar backscatter and rainwater storage is analyzed for a variety of radar configurations. The analysis is performed with a physical model, due to lack of detailed observations. To secure the soundness of this theoretical approach, the model is first validated with

small-scale radar measurements of a single tree and the final result is compared with large-scale observations. The simulations are restricted to temperate deciduous forest, because this is a promising forest type: observed backscatter changes after rain were largest for deciduous forest and this biome occurs in regions with humid and semihumid climates [19]. As forests differ from each other, the simulations are executed for four deciduous tree species, above a dry and wet soil, to account for differences in forest structure and soil moisture. The results of this analysis may also be used to assess the influence of rain, fog, or dew upon the radar applications that are mentioned in the first paragraph of this introduction.

II. MODELS

The theoretical base for simulating backscatter from rain-wetted vegetation was laid in our previous work [11]: the dielectric constant of the rain-wetted vegetation parts can be calculated from the amount of rainwater storage on the surface of the leaves or branches and the amount of water inside the leaves or branches. The radar backscatter from the forest as a whole is simulated next with a radiative transfer model. The main models for these calculations will be described in this paragraph. This array of models is extended in the present study, because in-situ measurements of the amount of rainwater storage are very complicated [20]–[22]. The total amount of rainwater storage in the tree is instead modeled from precipitation by [23]

$$S = S_{sat} \left[1 - e^{-kP_c/S_{sat}} \right] \quad (1)$$

where S is storage, or the total amount of rainwater that is retained on the surface of the plant, S_{sat} the saturation storage capacity and P_c cumulative precipitation, all in mm per unit ground area. The empirical factor k is set equal to $1 - p$, where p is the proportion of rain falling through the canopy. This equation is only valid when evaporation is low, thus during and shortly after rain. The saturation storage capacity is the maximum amount of storage that a plant can retain during rain. It is approximated by the maximum storage capacity, S_{max} , which is defined as the maximum amount of storage after a long rainstorm under calm weather conditions, when drainage from the canopy stopped [12]. The difference between these two parameters is the amount of rainwater that after rain drains from the plant under calm conditions (no wind), which is generally a small fraction of total storage [23]. The specific storage capacity, S_0 , is the maximum storage capacity per unit plant area. S_0 is given in mm and equals the waterfilm thickness on the surface of a leaf when the retained water is spread out evenly over one side of the leaf. S_{max} is calculated from S_0 of leaves, branches and trunks and their one-sided surface area A by [24]

$$S_{max} = \sum_i S_{0,i} A_i \quad (2)$$

where the subscript i stands for the entity: leaf, branch or trunk. $S_{0,i}$ may differ between species. For a given species, $S_{0,leaf}$ is generally lower than $S_{0,branch}$ and $S_{0,trunk}$ [24], [25]. S from (1) is scaled down to storage per unit plant area by substitution of S instead of S_{max} in (2). Under the assumption that each unit

plant area in the canopy has the same chance to get hit by a rain droplet [26], storage per unit plant area on leaves, branches, and trunks is even, till storage on leaves reaches $S_{0,leaf}$. Storage on branches and trunks is still lower than $S_{0,branch}$ and $S_{0,trunk}$ and additional storage is located on branches and trunks.

A second model relates the amount of storage per unit plant area on leaves and branches with backscatter by volumetric averaging of the dielectric properties of the retained water and the tree. The equations for calculating the dielectric constant of wet leaves are given. The dielectric constant of wet branches and trunks is calculated with the same approach.

The effective dielectric constant of a wet leaf is [11]

$$\epsilon_{wet\ leaf} = v_{dry\ leaf} \epsilon_{dry\ leaf} + v_{water} \epsilon_{water} \quad (3)$$

where v is the volume fraction and ϵ the complex dielectric constant. The effective thickness of the “leaf with waterfilm” entity increases with the thickness of the retained waterfilm on the surface of the leaf. The volume fractions of retained water v_{water} and the leaf $v_{dry\ leaf}$ are, respectively, the thickness of the waterfilm and that of the dry leaf, divided through the total thickness of the leaf with waterfilm. The water content inside the leaf determines the dielectric constant of the dry leaf. It is calculated with the Cole–Debye dual-dispersion model [27]

$$\epsilon_{dry\ leaf} = v_{bound} \epsilon_{bound} + v_{free} \epsilon_{free} + \epsilon_{residue} \quad (4)$$

where the subscript *bound* stands for water inside the leaf that cannot oscillate freely to the applied radarwave because it is bound to organic molecules and *free* for the free water inside the leaf. $\epsilon_{residue}$ accounts for a residual term due to solid matter inside the leaf. This term and the volume fractions are calculated from the gravimetric fraction water of the leaf, M_g , by [27]

$$v_{bound} = \frac{4.64M_g^2}{(1 + 7.36M_g^2)} \quad (5)$$

$$v_{free} = M_g (0.55M_g - 0.076) \quad (6)$$

$$\epsilon_{residue} = 1.7 - 0.74M_g + 6.16M_g^2. \quad (7)$$

The dielectric constant of bound water is calculated as a function of the radar frequency by [27]

$$\epsilon_{bound} = 2.9 + \frac{55}{1 + \left(\frac{jf}{0.18}\right)^{0.5}}. \quad (8)$$

The dielectric constant of water at a temperature of 10 °C (the averaged air temperature during the validation measurements) is [28]

$$\epsilon_{free} = 4.9 + \frac{79.1}{1 + \frac{jf}{12.6}} - j \frac{18\sigma}{f} \quad (9)$$

where f is the frequency in GHz and σ the ionic conductivity of the free water inside the leaf. The ionic conductance has a value of 1.27. The dielectric constant of intercepted rain, ϵ_{water} , is also calculated with (9). Retained rainwater is assumed to be pure and therefore $\sigma = 0$.

Forest backscatter is finally simulated with a radiative transfer model [29]. The forest is schematised as an assemblage of dielectric disks and cylinders with a given orientation,

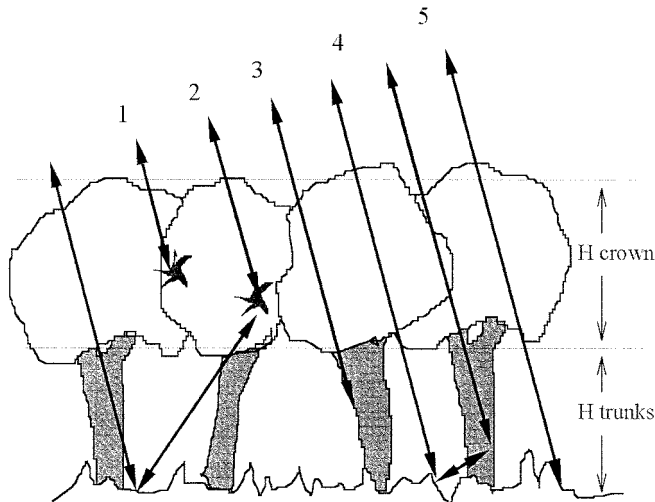


Fig. 1. Geometry of a forest canopy and the backscattering pathways in the first-order solution mode of the radiative transfer model: (1) crown scattering, (2) crown-ground interaction, (3) trunk scattering, (4) trunk-ground interaction, and (5) ground scattering. This figure is drawn after [29].

organized in maximal three horizontal layers. Disks represent leaves and cylinder branches and trunks. The model accounts for the first-order backscatter pathways of Fig. 1. Second-order scattering calculations (e.g., soil-trunk-leaf) demands extensive computational resources and only contributes to the absolute value of cross-polarized scattering [29], [30]. This study aims at the backscatter difference for a large number of forest situations and therefore second-order scattering is ignored. The soil backscatter is calculated with the integral equation model [31], using a soil dielectric constant determined by soil moisture content and soil composition [32].

III. VALIDATION

The models are validated with radar measurements of a single tree exposed to rain. This procedure is described in three parts. First, the radar measurements. These measurements are only briefly described as details can be found elsewhere [33], [34]. The next paragraph is about the collection of input data in order to run the models. The final part of this section describes the model simulations.

A. Radar Measurement

The measurements have been conducted at the experimental field of the University of Groningen, the Netherlands ($6^{\circ} 40' \text{ E}$, $53^{\circ} 10' \text{ N}$). Fig. 2 is a sketch of the experimental set-up. The tree was a mature ash (*Fraxinus excelsior*), 20 m tall. The foliage formed a 3–4 m thick surface layer around the centre of the tree. The tree branched out just above the ground and at breast height 12 stems were present. The radar was a ground-based FM-CW radar, built by METEK GmbH, Elsmhorn, Germany. The operation frequency was 10.4 GHz (X-band) and the polarization vertical. The radar was located at 60 m from the tree centre and pointed at the leafy upper-canopy. The beam width was 3° . A weather station was installed halfway the radar and the tree. Data of the first week of October 1999 were processed. A datalogger recorded the 5-min-averaged radar backscatter in linear units. To secure that the recorded data were the average of

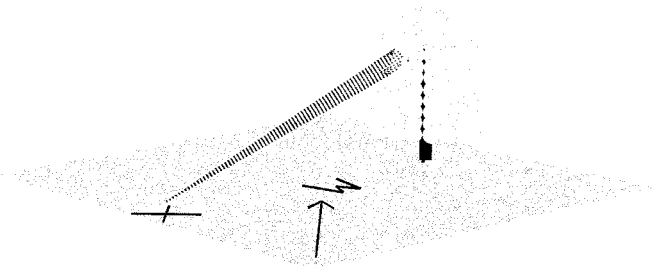


Fig. 2. Sketch of the experiment with the location of the X-band radar (X), weather station (W), and the tree. The arrow points at the wind direction during the experiment. The radar observed the wind exposed side of the tree.

independent samples (and fading was excluded) measurements with wind-driven tree motion were only processed. This motion was secured by applying a threshold on the Doppler shift in the reflected signal. The backscatter in linear units was converted to dB. The mean backscatter of the dry tree was set at 0 dB. The wetness of the tree was assessed with wetness sensors in the crown of the tree and at the weather station. A rainstorm was defined as being preceded by at least one hour of “no rain,” to allow the tree to dry from previous rainstorms. The recorded backscatter of 14 storms passed the data selection. To reduce scatter in the data, backscatter was averaged over all rainstorms. The number of storms that exceeded 1, 2, or 3 mm were 10, 7, and 2, respectively. The backscatter data recorded after 3 mm rain were excluded because of the low number of storms that exceeded 3 mm.

B. Tree Measurement

The model requires density, geometrical and dielectric data from the tree parts to simulate radar backscatter. The large-scale structure of the ash was a thin surface layer with a high density of leaves and branches, which surrounded an inner region with mainly trunks and major branches. The ground-based radar observed a cross-section with dense foliage. In the model, downward-looking radar observes a closed canopy. Because an ash has only sun leaves and no shade leaves, we assumed that the sides of the trees are not foliated in a closed canopy forest. Therefore, the schematised ash forest was assigned a crown and trunk height representative for the centre of the solitary tree. The heights were 3.5 m and 16.5 m, respectively. This was measured on photographs of the tree before and after leaf fall. It was assumed that the throughfall fraction p equalled the gap fraction in the canopy for light transmission. The latter parameter was determined on photographs of the ash: it was 0.23. The value of k was consequently 0.77.

The small-scale dimensions of the tree parts were derived as follows. An ash has pinnate leaves with seven to 13 separate leaflets, attached to a long, central nerve. The central nerve and the attached leaflets were the smallest entities in the simulations; the leaf itself was not regarded as an entity. The number density was estimated by counting the leaflets, nerves and secondary branches present at the end of a primary branch and dividing the numbers through the sampled volume, $\sim 0.94 \text{ m}^3$. This part was representative for the surface layer that contained the foliage. The dimensions from 543 leaflets, 107 nerves, and 17 secondary branches were measured. The leaflet length was

measured and related to leaflet area with a regression equation ($area = 1.05 \times length^{2.72}$, $R^2 = 0.98$, $n = 40$). The leaflets were divided into five classes to avoid frequency-dependent oscillations in the simulations. The density and dimensions of the large branches and trunks were obtained from field measurements and photographs taken after leaffall. The orientation of trunks, branches and leaves is described in the model by a probability density function (pdf), which is a sine or cosine function of the angle β with the vertical normal [29]. The pdfs of the trunks and branches were derived from photographs taken after leaffall. The pdf's were fitted to histograms that described the orientation of the branches and trunks in classes of 10° . The visual impression was that the orientation of trunks and branches did not change after the tree shed its leaves. Leaves were assigned a $\sin \beta$ orientation such that the direction in which the normal to the leaf surface is oriented is uniformly distributed over a spherical surface [30].

The gravimetric fraction water of leaflets, M_g , was determined by the difference in weight of fresh and oven-dried leaves. The leaves were picked from the lower branches. The M_g varied between 0.59 and 0.65. The slightly low value of $M_g = 0.60$ was used to calculate the dielectric constant because the radar observed the top of the ash and measurements in another ash indicated that the water potential in the top of an ash is lower than that at lower branches [35]. Branches and trunks were assigned the same water content. This value was found to be representative for the outer 0.5 cm of the trunks and branches. The specific storage capacity of leaflets, $S_{0,leaflet}$, was determined for 40 leaflets according to [25]. The method was as follows: after the determination of the fresh weight, each leaflet was submersed in water for 20 s. The droplet at the tip of the leaflet was removed with a blotting paper to simulate wind driven shake-off and the wet weight of the leaflet was determined. $S_{0,leaflet}$ was finally calculated by dividing the wet and dry leaflet weight difference through the one-sided area of the leaflet. The averaged value of $S_{0,leaflet}$ was 0.06 mm and the standard deviation 0.016 mm. These values are representative for the amount of storage when excess water drained. The $S_{0,branch}$ and $S_{0,nerves}$ were acquired by submersion of 20 nerves and 20 small branches for 1 min [36]. The area of the branches and nerves was calculated from their length and radius. $S_{0,trunk}$ was taken equal to that of the branches. The combined results are summarized in Table I.

C. Simulations

Firstly, the backscatter processes were simulated under conditions of a canopy that becomes wet during rain. Fig. 3 shows the vertical polarized X-band backscatter and the contributions of leaflets, nerves and branches as a function of rainwater storage. Trunks and soil were not included in these simulations, because the ground-based radar only observed the densely foliated upper canopy, where the trunks had approximately the same radius as the branches. The contribution of leaflets dominated total backscatter. With increasing storage, backscatter from leaflets increased and backscatter from branches and nerves simultaneously decreased, due to enhanced attenuation by wet leaves. Backscatter from leaflets increased until storage per unit plant area reached the maximum storage on leaflets, at $S_{0,leaflet} =$

TABLE I
MODEL INPUT FOR THE ASH SIMULATIONS. THE ACQUISITION OF THESE PARAMETERS IS DESCRIBED IN THE TEXT. THE BRANCHES AND LEAVES WERE PRESENT IN A 3.5-M-THICK FOLIAGE LAYER, THE TRUNKS IN A 16.5-M-THICK TRUNK LAYER. ADDITIONAL INPUT DATA ARE $M_g = 0.6$ AND $k = 0.77$. THE SPECIFIC STORAGE CAPACITY OF LEAFLETS IS DETERMINED IN THE LABORATORY (FIRST VALUE) AND BY ADJUSTING THE MODEL (SECOND VALUE)

	radius (m)	thickness (cm)/ length (m)	density (m^{-3})	orientation (pdf)	specific storage capacity (mm)
Leaflet 1	$1.9 \cdot 10^{-3}$	0.005	65	$\sin \beta$	0.06 / 0.09
Leaflet 2	$6.8 \cdot 10^{-3}$	0.005	260	$\sin \beta$	0.06 / 0.09
Leaflet 3	$1.3 \cdot 10^{-2}$	0.010	553	$\sin \beta$	0.06 / 0.09
Leaflet 4	$2.1 \cdot 10^{-2}$	0.015	505	$\sin \beta$	0.06 / 0.09
Leaflet 5	$3.0 \cdot 10^{-2}$	0.020	260	$\sin \beta$	0.06 / 0.09
Nerve	$5.5 \cdot 10^{-4}$	0.13	220	$\sin \beta$	0.09
Branch 1	$8.0 \cdot 10^{-3}$	2.00	1.1	$\cos^4 \beta$	0.21
Branch 2	$3.6 \cdot 10^{-3}$	0.38	18.1	$\sin^2 2\beta$	0.21
Trunk	$7.9 \cdot 10^{-2}$	16.5	$2.9 \cdot 10^3$	$\cos \beta$, $0^\circ < \beta < 15^\circ$	0.21

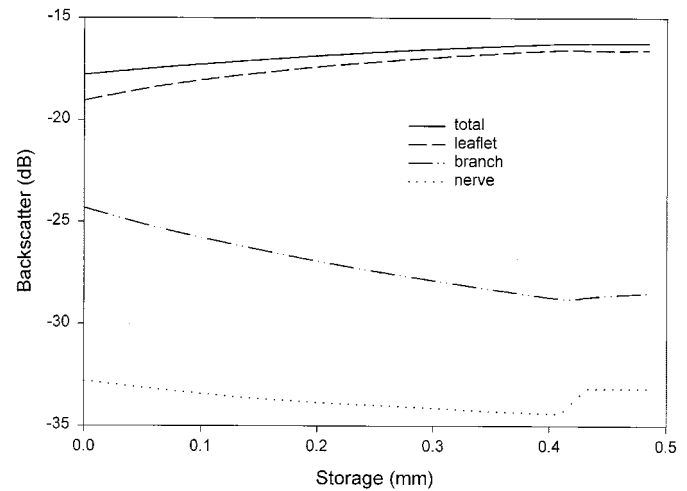


Fig. 3. The simulated vertical polarized X-band backscatter as a function of the amount of retained rain. The total backscatter is the sum of the contributions from leaflets, nerves and branches in linear units. This sum is next converted to the logarithmic decibel scale. The leaflets can not retain more water after 0.41 mm is stored and additional storage is located on the surface of branches and nerves. This additional storage hardly influenced total backscatter.

0.06 mm. This happened when total storage S was 0.41 mm. Nerves and branches were not yet saturated with rainwater and retained additional storage. Nerve backscatter increased more than branch backscatter by this additional storage, because the dielectric constant of wet nerves increased more than that of the branches. This is logical because the effective dielectric constant is the volumetric average of the dielectric constant of the dry nerve or branch and that of the retained rainwater. Both nerves and branches had an equal thick waterfilm on their surface, while the volume of the nerves was smaller than the volume of branches. On the other hand, the increased backscatter from nerves and branches hardly influenced total backscatter, because this backscatter was dominated by leaflet backscatter.

The simulations were compared with the measurements after transforming storage to precipitation with (1) and setting the backscatter of the dry tree at 0 dB (Fig. 4). The correlation between simulations and measurements was high, $R^2 = 0.84$, especially in the early stages of the rain storms ($P_e < 1.8$ mm, $R^2 = 0.93$). The simulated backscatter increase was lower than the measured backscatter increase. The correlation between simulations and measurements improved when the

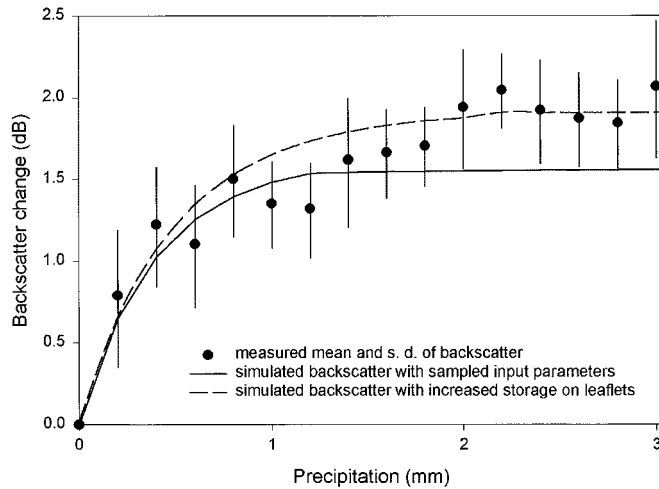


Fig. 4. Measured and simulated vertical polarized X-band backscatter change of the experimental tree as a function of cumulative precipitation. The measurements are the average of 14 rainstorms. The original simulation is performed with sampled input parameters. The second simulation is executed by increasing the water storage on leaflets with 50% till 0.09 mm per unit one-sided leaf area.

value of $S_{0,leaflet}$ was increased from 0.06 mm till 0.09 mm ($R^2 = 0.90$). We chose to increase $S_{0,leaflet}$ because the previous simulations indicated that the total backscatter was dominated by backscatter from leaflets. The original value of $S_{0,leaflet}$ was determined under laboratory conditions. The radar observations were made during rain. The laboratory determinations of $S_{0,leaflet}$ were representative for the amount of storage after rain, when drainage of excess water ended. The radar observations were made during rain. Therefore, the amount of storage on the surface of leaves during rain could be higher than the laboratory determined value.

Other processes may also change the modeled sensitivity of radar backscatter to rainwater storage on the surface of leaves. Some of these processes will be discussed in this paragraph. The water content of leaves was assumed to be relatively low, $M_g = 60\%$. The influence of this parameter on the radar backscatter sensitivity to rainwater storage has been investigated by two simulations. The first simulation assumed $M_g = 65\%$, for both dry and wet leaves. This simulation resulted in a 0.3 dB lower backscatter change due to wetting. In other words, the discrepancy between the measured and modeled backscatter increased by assuming a higher water content of the leaves. The second simulation assumed that the water content inside the leaves increased during wetting of the tree, because liquid water practically blocks stomata and transpiration of leaves may stop [37]. When the gravimetric water content of the leaves was increased from 60% to 65% during wetting of leaves, the modeled radar sensitivity to precipitation appeared to be only 0.1 dB higher than the previous simulations. The reason for this low sensitivity to the internal water content of the leaves was that the dielectric constant of the wet leaves was dominated by the waterfilm on surface of the leaves and not by the internal water content of the leaf. The waterfilm on the surface of leaves was assumed to be pure water, but it might be little saline. This salinity might influence the radar backscatter processes. Rainwater is expected to have a lower salinity than the water inside leaves, or $\sigma < 1.27$,

because elements like Na^+ and K^+ may leach from the interior of leaves to the waterfilm on the surface of leaves [38]. According to (9), a suchlike salinity ($\sigma < 1.27$) of rainwater hardly influences the dielectric constant of water at high frequencies. Finally, the orientation of wet leaves could change due to the larger weight of wet leaves. This was not expected to be important because only measurements with wind-driven tree motion were used.

Therefore, the most likely explanation for the discrepancy between the measured and simulated backscatter change is the underestimation of the amount of rainwater storage on the surface of leaves. However, in the discussion we will come back whether the large increase (50%) in the amount of rainwater storage on leaves during rain is realistic.

IV. SENSITIVITY ANALYSIS

After the model validation with small-scale radar measurements, the model was applied in a theoretical analysis to relate the sensitivity of satellite radar to rainwater storage in an arbitrarily deciduous forest. Forest structure and soil moisture varies within a forest. The influence of forest structure was taken into account by calculation of the backscatter change between a wet and dry forest for four different single species forests. The species were: a beech (*Fagus sylvatica*), two poplar species (the euramerican clone *Populus robusta* and *Populus balsamifera*) and an ash (*Fraxinus excelsior*). These species were chosen from the most abundant species in a temperate deciduous forest [19]. Undergrowth was ignored because this was assumed to be insignificant under a closed canopy. Storage in each tree was calculated by assignment of an equal thick waterfilm on leaves (0.09 mm), branches and trunks (0.21 mm), based on the ash schematizations. As will be argued in the discussion, the maximum waterfilm thickness on the surface of leaves and hence the maximum backscatter change, is in the same order of magnitude for the simulated tree species. The dielectric constant of all vegetated parts was calculated from $M_g = 0.6$.

Soil moisture variations were taken into account by execution of the simulations for three different states of soil wetness: a soil that remains dry or wet and a soil in which wetness increased when the canopy intercepted rain. The dry and the wet soil were assigned a volumetric water content of 10 and 20%. This difference in soil moisture content was higher than observed in the top 5 cm of bare soils during and in the first five days after several rain events in the Netherlands [39]. We applied this “worst-case scenario” to compensate for uncertainties in soil reflection modeling, because the influence of surface roughness upon radar backscatter is very complicated. Describing the surface roughness by root-mean-square (*rms*) height and correlation length is only a simple approximation [40]. It was for example found that the *rms* height and correlation length increased when sampled over longer transects [41]. The values we used (*rms* height 1 cm, correlation length 4 cm) were based on an Alaskan forest soil [9]. Such a soil is smooth at L-band and rough at C- and X-band (Fraunhofer-criterion, [42]). Similar values (*rms* height 1.2, correlation length 5 cm) have been used for analysing the backscatter of an Amazonian floodplain forest in a sensitivity

TABLE II

TREE AND SOIL PROPERTIES USED FOR THE SENSITIVITY ANALYSIS SIMULATIONS. ALL TREES ARE DECIDUOUS AND ABUNDANT IN TEMPERATE DECIDUOUS FORESTS. NOTE THE VARIATION IN TREE HEIGHT, STEM DENSITY AND LEAF AREA INDEX

	Canopy			
	poplar (<i>P. robusta</i>)	poplar (<i>P. balsamifera</i>)	beech (<i>F. sylvatica</i>)	ash (<i>F. excelsior</i>)
Height (m)	17.1	30.2	14.5	20
Height foliage layer (m)	11.4	10.1	3	3.5
Stem density (stems.ha ⁻¹)	217	1060	500	478
Leaf area index	2.8	3.6	6.7	6.2
Stem diameter (cm)	26	22.5	8	15
Thickness leaves (cm)	0.022	0.030	0.013	0.016
<i>S</i> (mm)	0.33	0.64	0.73	0.73
<i>S</i> leaves only (mm)	0.23	0.33	0.60	0.56
Source	[53]	[9]	[10]	This study
Soil				
Water content	10 vol. % (dry), 20 vol. % (wet)			
Composition	10% sand, 40% silt, 50% clay			
Surface roughness	<i>rms</i> height 1 cm, correlation length 4 cm (over a transect of 1 m)			

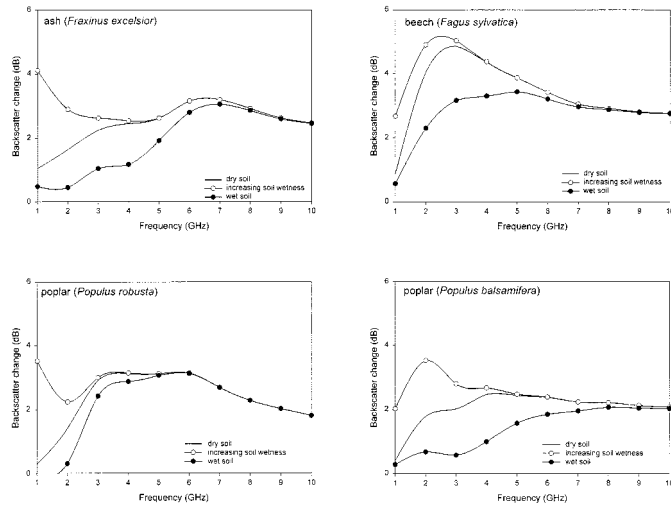


Fig. 5. The simulated backscatter change between a wet and a dry tree for four different tree species above three different soils as a function of frequency for a *vv*-polarized radar with $\theta = 20^\circ$. All wet trees were assigned a waterfilm thickness of 0.09 mm on one side of the leaves. Differences between the simulations are therefore solely caused by differences in forest structure and soil moisture content.

analysis over the same range of frequencies and incidence angles as this study [43]. Aggregate properties of the forest stands are given in Table II.

Next to varying forest structure and soil moisture content, the simulations were executed for different radar configurations. The radar configurations were simulated by varying the frequency f (1–10 GHz), incidence angle θ (20–60°) and polarization (vertical, *vv*, horizontal, *hh*, or cross-polarized, *hv*) of the radarbeam. The values of f and θ were chosen to include most present and proposed imaging satellite radars [44].

A. Influence of Tree Species and Soil Moisture

The simulations for a radar with one incidence angle ($\theta = 20^\circ$) and polarization (*vv*) are highlighted to demonstrate the variability caused by the tree species and soil moisture (Fig. 5). It is emphasised that the simulated backscatter difference between a wet and a dry canopy is the slope of the relation between storage per unit plant area and backscatter, because each species was assigned an equal thick waterfilm on leaves, branches and trunks. This waterfilm thickness may

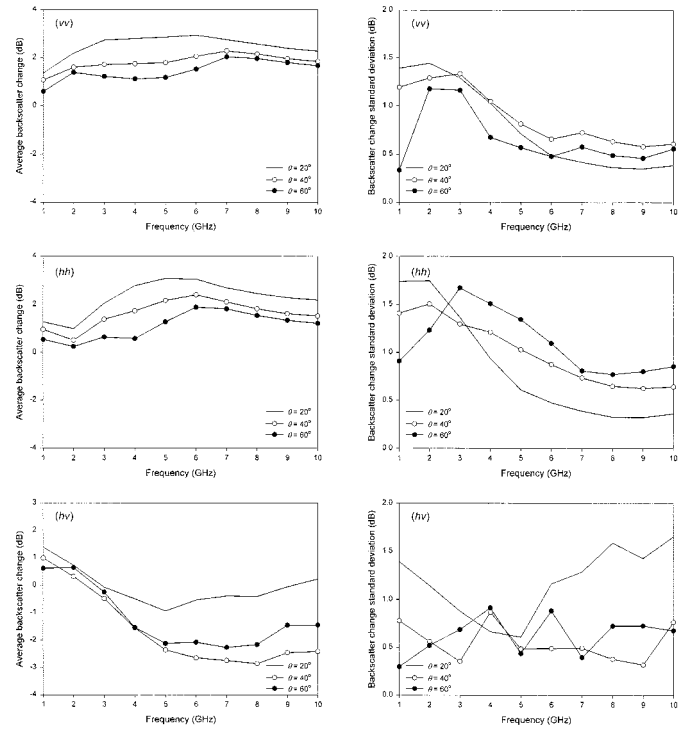


Fig. 6. The average and standard deviation of the simulated backscatter change due to rainwater storage of four different forest trees above three different soils as a function of the radar configuration. The figures are organized according to the polarization direction of the radar, which are from top till bottom a vertical, horizontal, and cross polarization. Again, each wet tree had a waterfilm thickness of 0.09 mm on the surface of leaves.

differ slightly from the maximum waterfilm thickness, which is unique for each species. The simulated backscatter change differed largely between the forests at low frequencies. These large differences were caused by the variable contribution of soil backscatter to total backscatter. Backscatter increased most when wetness of both soil and canopy increased. Backscatter change was least when the soil was already wet under the dry canopy, because the relatively large contribution of wet soil backscatter to total backscatter strongly reduced the radar sensitivity to storage. The contribution of soil backscatter to total backscatter reduced at frequencies above 6 GHz and the differences in simulated backscatter change became small, within 1 dB. These differences were caused by the forest stand structure. At 10 GHz, the highest backscatter change was simulated for the ash and beech stand, which had the thinnest leaves and consequently the highest dielectric constants of wet leaves (the dielectric constant of wet leaves was calculated as the volumetric average of the dielectric constant of the dry leaf and the waterfilm on the surface, which had the same thickness in all simulations).

B. Influence of Radar Configuration

For each radar configuration, the backscatter change due to storage was calculated for 4 tree species \times 3 states of soil wetness = 12 unique forests. Per radar configuration, the results of these 12 simulations were averaged to estimate the sensitivity of backscatter to rainwater storage in an arbitrarily forest (Fig. 6). The averaged backscatter increased when the forest

became wet, except for simulated hv -polarized backscatter, which decreased when the forest became wet. According to the model, hv -backscatter was dominated by backscatter from branches. When leaves became wet, they strongly attenuated the backscatter from branches and the simulated total backscatter decreased. The maximal change was simulated for hh -, vv - and hv -polarization at, respectively, 5, 6, and 8 GHz. This maximum appeared at steep incidence angles, except for hv -polarization, where it appeared at $\theta = 40^\circ$. In all cases, the absolute value of the maximal change was in the same order of magnitude, 3 dB. The averaged backscatter change for a radar with hv -polarization, $\theta = 20^\circ$, was close to 0 dB and it strongly depended upon the species. This strong dependency of backscatter upon the species resulted in a large standard deviation. The standard deviation of the other radar configurations was large at low frequencies, when soil backscatter was most influencing. The standard deviation decreased with increasing frequency, till a minimum was reached at 8–9 GHz. The sign and order of magnitude of the simulated backscatter change were in agreement with the observations mentioned in the introduction, maximal +3 dB at C-band and +1 dB at L-band, except for hv -polarized backscatter, where observations and simulations had an opposite sign.

V. DISCUSSION

The objective of this study was to assess whether rainwater storage in deciduous forests could be retrieved quantitatively with imaging satellite radar. The approach was simulating the backscatter change due to rainwater storage in the canopy of trees for a number of forest tree species, after a validation of the model. Quantitative aspects of the validation and sensitivity analysis are first discussed. The results are next evaluated with large-scale observations. The main research question is addressed at the end of this discussion.

A. Validation

The model was validated with radar measurements of a single tree. The input data for the waterfilm thickness on the surface of leaves was determined in the laboratory. The correlation between simulations and measurements improved by increasing the waterfilm thickness on leaves with 50%. Unfortunately, we did not find any measurements of the waterfilm thickness on the surface of ash leaves during wetting. Instead, indirect evidence that justifies this increase will be discussed. The waterfilm was determined in the laboratory by weighting a fresh leaflet, submersing it in water, removing the drop at tip of the leaflet with a blotting paper, and reweighting the wet leaflet. This determination resulted in the amount of retained water when gravimetric and retentional forces were in static equilibrium and excess water was removed. On the other hand, the radar measurements were performed during the first stages of rainstorms, when the tree moved in the wind. Physical models suggest that in the first stage of a rainstorm extra water is retained on the surface of leaves before equilibrium develops and excess water drains to the ground [45]. The best available direct measurements for a comparison of the amount of rain water storage on the surface of leaves during and after rain

(when drainage of excess water ended), were acquired by wetting plants or plant parts in the laboratory and measuring the plant weight before, during and after wetting. The amount of water storage on coyote bush (*Baccharis pilularis*) during spraying with water was 47% higher than the amount of water storage after spraying and drainage of excess water ended [46]. For five eucalyptus species, the amount of water storage on the surface of leaves during simulated rainfall was 15–30% higher than the amount of water storage after drainage stopped [23]. Exceptions were *E. maculata*, which had a 50% higher storage during simulated rain and *Acacia longiflora*, which had a 70% higher storage during simulated rain. Further evidence was provided by [47]. The waterfilm thickness on leaves was determined for a number of alpine species by two different methods. The first method was identical to our method. The second method was that complete specimen were wetted with a rainfall simulator. All excess water was immediately after wetting stopped removed by shaking. This amount of excess water that could drain was scaled down to the waterfilm thickness on leaves. The second method resulted in a larger $S_{0,leaf}$ than the first method. The difference was even up to an order of magnitude. It is concluded that during rain the storage on the surface of leaves could be 50% higher than after rain and underestimation of waterfilm thickness in the laboratory is a plausible explanation for the difference between model and measurement. Therefore, radar appears to be suitable for quantifying storage in a deciduous tree canopy, on condition that detailed data on forest structure and weather are available.

B. Sensitivity Analysis

The sensitivity to storage in a temperate deciduous forest was next assessed by simulation of the backscatter of four forest stands. Storage in these stands was calculated by extrapolating the values of $S_{0,leaf}$ and $S_{0,trunk}$ from the ash to the other species. It will be discussed whether this extrapolated storage approximated the maximal or saturation storage for each species and the simulated backscatter change is consequently the maximum backscatter change for all tree species. Measurements of S_0 or S_{sat} were, again, not available for the modeled species and therefore, stand aggregate values of S (see Table II) were compared with published values of S_{max} . The maximum storage capacity of a poplar stand was 0.40–0.66 mm in summer and 0.20–0.39 mm in winter [48]. The LAI of this stand was 3.5. Under the assumption that the difference in maximum storage between summer and winter could be attributed to rainwater retention on leaves, the maximum waterfilm thickness on the surface of poplar leaves had to be at least 0.06–0.08 mm, in agreement with the used value. Maximum storage after rain stopped of two mature beech stands was 0.5 and 0.8 mm in winter and 1.2 and 1.3 mm in summer [49], [50]. Both observations indicated that storage on leaves in a beech stand is in the order of 0.5–0.7 mm, also in agreement with the simulations. On the other hand, measured wintertime storage strongly deviated from modeled storage on branches and trunks, indicating that $S_{0,branch}$ and $S_{0,trunk}$ differ between species. Differences in $S_{0,branch}$ and $S_{0,trunk}$ influenced simulated backscatter change hardly, because the volume of retained water on branches and trunks was several

orders of magnitude smaller than the branch or trunk volume. The dielectric constant of wet branches consequently approximated the dielectric constant of dry branches. Recapturing, the maximum storage capacity per unit plant area of leaves, $S_{0,leaf}$, was in the same order of magnitude for all simulated species. The simulated rainwater storage on leaves approximated this maximal value. The simulated backscatter change between a wet and a dry tree therefore equals the maximum backscatter change due to storage for each tree species. The simulated species are abundant in temperate deciduous forests. It is therefore concluded that the simulated average backscatter change is indicative for the theoretical maximal backscatter sensitivity to storage in an arbitrarily temperate deciduous forest.

C. Observations

The quality of the simulations was evaluated by going back to the observations that were mentioned in the introduction. Just after rain, the AIRSAR observed backscatter of a forest increased with +1–2 dB at L-band and with +2–3 dB at C-band for all polarization directions [7]. The modeled co-polarized backscatter change was in agreement with these observations. Modeled cross-polarized backscatter change contradicted the observations, because it decreased. According to the model, hv -backscatter was dominated by backscatter from branches. The backscatter from the branches decreased due to enhanced attenuation of wet leaves. The branch backscatter decrease was more important than the backscatter increase from wet leaves. We therefore expect that hv -backscatter from leaves was underestimated by the model. Experimental evidence was not found for this hypothesis. Without additional experiments, a statement on the sensitivity of cross-polarized backscatter to storage cannot be made. The other observations of wet deciduous forest were made with the radar of the ERS-satellite [9], [10]. The backscatter increased with 1.5–2 dB when the forest became wet. This value was slightly lower than the simulated backscatter increase. Two reasons can explain the difference: 1) part of the stored rainwater was evaporated, or 2) due to the steep incidence angle of the ERS-radar, $\theta = 23^\circ$, some direct soil backscatter was received through gaps in the canopy. A large contribution of soil backscatter to total backscatter weakens the sensitivity to storage. Radar with a flatter incidence angle would receive less direct backscatter from the soil, because the radar wave has to pass a longer path of vegetation before being reflected at the soil. It is therefore expected that for natural forests the sensitivity of a co-polarized radar with $\theta = 20^\circ$ is reduced till it approximates that of a co-polarized radar with $\theta = 40^\circ$. The theoretical sensitivity to storage is therefore assessed to be $2 \text{ dB} \pm 0.75 \text{ db}$ for a co-polarized C- or X-band radar and $1 \text{ dB} \pm 1.25 \text{ db}$ for an L-band radar.

D. Feasibility of Storage Retrieval From Satellite Radar Data

Given the theoretical sensitivity of radar backscatter to rainwater storage in temperate deciduous forests, is storage retrieval feasible from data acquired by present or future imaging satellite radar?

Presently available data are recorded with the ERS or RADARSAT satellite, which have a C-band radar with one polarization direction. The measurement precision of such a radar generally is within 1 dB [51]. Taking this additional uncertainty into account, the sensitivity to rainwater storage will be in the order of $2 \text{ dB} \pm 1 \text{ db}$, which results in an error of 50% in retrieved wetness. This waterfilm thickness has to be extrapolated to total storage in a canopy. Due to the large uncertainty, a feasible application of the current satellites might be restricted to distinguish wet and dry parts in a large forest. However, a satellite image contains spatial information. This spatial information could contain valuable information on the evaporation of rainwater storage in the canopy of trees. Rainstorms generally move over an area. On condition that the rainstorm motion is known (e.g., observed by ground-based rainradar), the duration of canopy wetness after a rainstorm could be deduced from ERS or RADARSAT images.

The next generation satellites may acquire vv , hh , and hv -polarized C-band images simultaneously (RADARSAT-2, expected launch late 2003). It has been demonstrated that the dielectric constant of a forest canopy can be estimated elegantly from multiple polarized radar data [4], [52]. The coverage access of RADARSAT-2 at equator is every 2–3 days and above 70° latitude daily. The coverage access of RADARSAT-2 will be higher when the left- and right-looking capability is taken into account. RADARSAT-2 is modified to support a proposed tandem mission with RADARSAT-3. With such a high temporal coverage and on condition that additional rainfall data are available, it is possible to distinguish observations of wet days from a baseline containing observations of dry days. Changes in forest structure and soil moisture content will be visible in the dry day baseline. The backscatter change between the observations made on wet days and on dry days can be interpreted in terms of forest wetness. We therefore expect that the retrieval of the amount of rainwater storage in deciduous forests will improve with the launch of the next generation radar satellites.

ACKNOWLEDGMENT

The authors would like to thank Dr. C. Proisy and two anonymous referees for their comments on the manuscript.

REFERENCES

- [1] L. L. Hess, J. M. Melack, and D. S. Simonette, "Radar detection of flooding beneath the forest canopy: A review," *Int. J. Remote Sensing*, vol. 5, pp. 1313–1325, 1990.
- [2] M. C. Dobson, F. W. Ulaby, L. E. Pierce, T. L. Sharik, K. M. Bergen, J. Kellndorfer, J. R. Kendra, E. Li, Y. C. Lin, A. Nashashibi, K. Sarabandi, and P. Siqueira, "Estimation of forest biophysical characteristics in Northern Michigan with SIR-C/X-SAR," *IEEE Trans. Geosci. Remote Sensing*, vol. 33, pp. 877–895, July 1995.
- [3] J. T. Pulliainen, P. T. Mikkela, M. T. Hallikainen, and J. P. Ikonen, "Seasonal dynamics of C-band backscatter of boreal forest with applications to biomass and soil moisture estimation," *IEEE Trans. Geosci. Remote Sensing*, vol. 34, pp. 758–769, May 1996.
- [4] M. Moghaddam and S. S. Saatchi, "Monitoring tree moisture using an estimation algorithm applied to SAR data from boreas," *IEEE Trans. Geosci. Remote Sensing*, vol. 37, pp. 901–916, May 1999.
- [5] R. Bernard and D. Vidal-Madjar, "C-band radar cross section of the Guyana rain forest, possible use as reference target for spaceborne radars," *Remote Sens. Environ.*, vol. 27, pp. 25–36, 1989.

- [6] J. Way, J. Paris, E. Kasischke, C. Slaughter, L. Viereck, N. Christensen, M. C. Dobson, F. Ulaby, J. Richards, A. Milne, A. Sieber, F. J. Ahern, D. Simonett, R. Hoffer, M. Imhoff, and J. Weber, "The effect of changing environmental conditions on microwave signatures of forest ecosystems: Preliminary results of the March 1988 Alaskan aircraft SAR experiment," *Int. J. Remote Sensing*, vol. 11, pp. 1119–1144, 1990.
- [7] M. C. Dobson, L. Pierce, K. McDonald, and T. Sharik, "Seasonal change in radar backscatter from mixed conifer and hardwood forest in Northern Michigan," in *Proc. IGARSS 91*, 1991, pp. 1121–1124.
- [8] F. J. Ahern, D. J. Leckie, and J. A. Drieman, "Seasonal changes in relative C-band backscatter of northern forest cover types," *IEEE Trans. Geosci. Remote Sensing*, vol. 31, pp. 668–680, May 1993.
- [9] E. Rignot, J. B. Way, K. McDonald, L. Viereck, C. Williams, P. Adams, C. Payne, W. Wood, and J. Shi, "Monitoring of environmental conditions in Taiga forest using ERS-1 SAR," *Remote Sens. Environ.*, vol. 49, pp. 145–154, 1994.
- [10] C. Proisy, E. Mougin, E. Dufrene, and V. le Dantec, "Monitoring seasonal changes of a mixed temperate forest using ERS-SAR observations," *IEEE Trans. Geosci. Remote Sensing*, vol. 38, pp. 540–552, Jan. 2000.
- [11] J. J. M. De Jong, W. Klaassen, and A. Ballast, "Rain storage detected with ERS tandem mission Sar," *Remote Sensing Environ.*, vol. 72, pp. 170–180, 2000.
- [12] R. E. Horton, "Rainfall interception," *Month Weather Rev.*, vol. 47, pp. 603–623, 1919.
- [13] J. W. Shuttleworth, "Evaporation from Amazonian rain forest," in *Proc. R. Soc. London B*, vol. 233, 1988, pp. 321–346.
- [14] A. P. Pitman, A. Henderson-Sellers, and Z. L. Yang, "Sensitivity of regional climates to localized precipitation in global models," *Nature*, vol. 346, pp. 734–737, 1990.
- [15] E. A. B. Eltahir and R. L. Bras, "A description of rainfall interception over large areas," *J. Clim.*, vol. 6, pp. 1002–1008, 1993.
- [16] J. Noilhan, P. Lacarrère, A. J. Dolman, and E. M. Blyth, "Defining area-average parameters in meteorological models for land surfaces with mesoscale heterogeneity," *J. Hydrol.*, vol. 190, pp. 302–316, 1997.
- [17] S. J. Ghan, J. C. Liljegren, W. J. Shaw, J. H. Hubbe, and J. C. Doran, "Influence of subgrid variability on surface hydrology," *J. Clim.*, vol. 10, pp. 3157–3166, 1997.
- [18] W. L. Gates, A. Henderson-Sellers, G. J. Boer, C. K. Folland, A. Kitoh, B. J. McAvaney, F. Semazzi, N. Smith, A. J. Weaver, and Q. C. Zeng, "Climate models-evaluation," in *Climate Change 1995, The Science of Climate Change*. Cambridge, U.K.: Cambridge Univ. Press, 1996, Intergovernmental Panel on Climate Change, pp. 279–284.
- [19] E. Röhrig and B. Ulrich, *Temperate Deciduous Forests*. Amsterdam, The Netherlands: Elsevier, 1991.
- [20] I. R. Calder and Wright, "Gamma ray attenuation studies of interception from sitka spruce: Some evidence for an additional transport mechanism," *Water Resources Res.*, vol. 22, pp. 409–417, 1986.
- [21] W. Bouten, P. J. F. Swart, and E. Water, "Microwave transmission, a new tool in forest hydrological research," *J. Hydrol.*, vol. 124, pp. 119–130, 1991.
- [22] Z. Thekshaimanot and P. G. Jarvis, "Direct measurement of evaporation of intercepted water from forest canopies," *J. Appl. Ecol.*, vol. 28, pp. 603–618, 1991.
- [23] A. R. Aston, "Rainfall interception by eight small trees," *J. Hydrol.*, vol. 42, pp. 383–396, 1979.
- [24] S. R. Herwitz, "Interception storage capacities of tropical rain forest trees," *J. Hydrol.*, vol. 77, pp. 237–252, 1985.
- [25] S. Liu, "Estimation of rainfall storage capacity in the canopies of cypress wetlands and slash pine uplands in North-Central Florida," *J. Hydrol.*, vol. 207, pp. 32–41, 1998.
- [26] I. R. Calder, "Dependence of rainfall interception on drop size: 1 development of the two layer stochastic model," *J. Hydrol.*, vol. 185, pp. 363–378, 1996.
- [27] F. T. Ulaby and M. A. EL-Rayes, "Microwave dielectric spectrum of vegetation—Part II: Dual-Dispersion model," *IEEE Trans. Geosci. Remote Sens.*, vol. GE-25, pp. 550–557, 1987.
- [28] A. Stogryn, "Equations for calculating the dielectric constant of saline water," *IEEE Trans. Microwave Theory Tech.*, vol. MTT-19, pp. 733–736, 1971.
- [29] M. A. Karam, A. K. Fung, R. H. Lang, and N. S. Chauhan, "A microwave scattering model for layered vegetation," *IEEE Trans. Geosci. Remote Sensing*, vol. 30, pp. 767–783, July 1992.
- [30] K. C. McDonald, M. C. Dobson, and F. T. Ulaby, "Modeling multifrequency diurnal backscatter from a walnut orchard," *IEEE Trans. Geosci. Remote Sensing*, vol. 29, pp. 852–863, Nov. 1991.
- [31] A. K. Fung, Z. Li, and K. S. Chen, "Backscattering from a randomly rough dielectric surface," *IEEE Trans. Geosci. Remote Sensing*, vol. 30, pp. 356–369, Mar. 1992.
- [32] H. T. Hallikainen, F. T. Ulaby, M. C. Dobson, M. A. El-Rayes, and L. K. Wu, "Microwave Dielectric behavior of wet soils," *IEEE Trans. Geosci. Remote Sensing*, vol. GE-23, pp. 25–34, 1985.
- [33] J. J. M. de Jong, H. W. de Groot, W. Klaassen, and P. J. C. Kuiper, "Radar backscatter change from an ash in relation from its hydrological properties," in *Proc. IGARSS 2000*, 2000, pp. 2927–2929.
- [34] —, "Radar measurement of rain storage in a deciduous tree," *J. Atmos. Ocean. Tech.*, submitted for publication.
- [35] H. Cochard, M. Peiffer, K. Le Gall, and A. Garnier, "Developmental control of xylem hydraulic resistances and vulnerability to embolism in *fraxinus excelsior* L.: Impacts on water relations," *J. Exp. Botany*, vol. 48, pp. 655–663, 1997.
- [36] N. J. M. Hutchings, R. Miline, and J. M. Crowther, "Canopy storage capacity and its vertical distribution in a sitka spruce canopy," *J. Hydrol.*, vol. 104, pp. 161–171, 1988.
- [37] M. Ishibashi and I. Terashima, "Effects of continuous leaf wetness on photosynthesis: Adverse aspects of rainfall," *Plant, Cell, Environ.*, vol. 18, pp. 431–438, 1995.
- [38] A. M. Gordon, C. Chourmouzis, and A. G. Gordon, "Nutrient inputs in litterfall and rainwater fluxes in 27-year old red, black and white spruce plantations in Central Ontario, Canada," *For. Ecol. Management*, vol. 138, pp. 65–78, 2000.
- [39] M. Borgeaud and N. Floury, "On the retrieval of soil moisture of bare soils with ERS SAR data," in *Proc. IGARSS*, 2000, pp. 1687–1689.
- [40] M. Zribi, V. Ciarletti, O. Taconet, J. Paillé, and P. Boissard, "Characterization of the soil structure and microwave backscatter based on numerical three dimensional surface representation: Analysis with a fractional brownian model," *Remote Sens. Environ.*, vol. 72, pp. 159–169, 2000.
- [41] M. Davidson, T. Le Toan, F. Mattia, T. Manninen, P. Borderies, I. Chenerie, and M. Borgeaud, "A validation of multi-scale roughness description for the modeling of radar backscatter from bare soil surfaces," in *Proc. Second int. Workshop Retrieval Bio-and Geo-Physical Parameters From Sar Data for Land Applications*, 1998, pp. 395–400.
- [42] F. T. Ulaby, R. K. Moore, and A. K. Fung, *Microwave Remote Sensing, Active and Passive*. Norwood, MA: Artech House, 1981, vol. II.
- [43] Y. Wang, L. L. Hess, S. Filoso, and J. M. Melack, "Understanding the radar backscatter from flooded and nonflooded Amazonian forests: Results from canopy backscatter modeling," *Remote Sens. Environ.*, vol. 54, pp. 324–332, 1995.
- [44] B. Huneycutt and J. Zuzek, "Frequency use and needs of spaceborne active sensors," in *Proc. IGARSS*, 2000, pp. 2457–2463.
- [45] A. J. Rutter, K. A. Kershaw, P. C. Robins, and A. J. Morton, "A predictive model of rainfall interception in forests: I. Derivation of the model from observations in a plantation of corsican pine," *Agric. Meteorol.*, vol. 9, pp. 367–384, 1971.
- [46] R. A. Grah and C. C. Wilson, "Some components of rainfall interception," *J. For.*, vol. 42, pp. 890–898, 1944.
- [47] R. K. Monson, M. C. Grant, C. H. Jaeger, and A. N. Schoettle, "Morphological issues for the retention of precipitation in the crown of alpine plants," *Environ. Exp. Bot.*, vol. 32, pp. 319–327, 1992.
- [48] J. A. Elbers, A. J. Dolman, E. J. Moors, and W. Snijder, "Hydrologie en waterhuishouding van bosgebieden in Nederland, fase 2: Meetopzet en eerste resultaten," Staring centrum, Wageningen, Netherlands, Rep. 333.2, 1996.
- [49] G. Kändler, "Die Ermittlung von Bestandesparametern als Eingangsgrößen für Interzeptionsmodelle mit Hilfe Aerophotogrammetrischer Verfahren," Freiburg, Germany, Mitteilungen des Frostl. Versuchs- und Forschungsanstalt Baden-Württemberg, no. 127, 1986.
- [50] G. Hörmann, A. Branding, T. Clemen, M. Herbst, A. Hinrichs, and F. Thamm, "Calculation and simulation of wind controlled canopy interception of a beach forest in Northern Germany," *Agric. For. Meteorol.*, vol. 79, pp. 131–148, 1996.
- [51] H. Laur, P. Bally, P. Meadows, J. Sanchez, B. Schaettler, and E. Lopinto, "Derivation of the Backscattering Coefficient σ^0 in ESA ERS SAR PRI Products," ESA, Noordwijk, The Netherlands, Document ES-TN-RS-PM-HL09, Issue 2, Rev. 4, 1997.
- [52] M. Moghaddam and S. S. Saatchi, "Estimation of vegetation variables using AIRSAR data containing multiple scattering mechanisms," in *Proc. IGARSS*, 2000, pp. 1408–1410.
- [53] D. H. Hoekman, M. van der Linden, and J. J. van der Sanden, "Application of ERS-1 SAR Data in Agriculture and Forestry," BCRS, Delft, The Netherlands, Rep. 94-34, G. J. A. Nieuwenhuis and W. W. L. van Rooij, Eds., 1995.



Joost J. M. de Jong (S'99) received the engineering degree in environmental sciences from Van Hall Institute, Groningen, The Netherlands, in 1997. He is currently pursuing the Ph.D. degree in mathematics and physical sciences at the University of Groningen.

His research interest are modeling and measuring of geochemical cycles, with emphasis on spatial aspects of biosphere–atmosphere exchange processes in forests and the use of remote sensing to monitor these processes.



Pieter J. C. Kuiper has been an Emeritus Professor at the University of Groningen (UG), The Netherlands, since 1999. He was a Full Professor of plant physiology for 25 years at UG. His main interest during this period was adaptation processes in plants to various stress conditions, including global change. More recently he included in his interest the interface between palaeobotany and ecophysiology of plants and aspects of the hydrological cycle of forests.



Wim Klaassen received the Ph.D. degree from the University of Utrecht on the propagation of radio waves in precipitation in 1989.

He is currently an Assistant Professor in meteorology, University of Groningen, Groningen, The Netherlands. His main research topics are the water use of forests and the influence of landscape patchiness on atmospheric exchange of wind, water, and air pollution. He recently extended his research to the biogenic regulation of ocean–atmosphere interaction.